Journal of Systems Smartening and Data Processing
Vol. 3 - No. 2 - Summer 2025

Comprehensive study of transformer inrush current mitigation techniques

Amir Ghaedi, ***Associate Professor***

Department of Electrical Engineering, Dariun Branch, Islamic Azad University, Dariun, Iran
Amir.ghaedi@iau.ac.ir

Received: 19 April 2025	**Revised:** 01 August 2025	**Accepted:** 16 August 2025

Abstract:

The transformer inrush current is the high amplitude and non-sinusoidal current occurred in the initial cycles after energizing the transformer. This current may result in some problems in the power system such as voltage drop, heat losses, power quality reduction and malfunction of the protective relays. To prevent malfunction of the protective system, the harmonic contain of this current is analyzed to recognize this current from the fault currents. However, the techniques that reduce the amplitude of the transformer inrush current can prevent from the disruptive effects of this current. For this purpose, in this paper a comprehensive study is performed on the novel techniques that can be used to mitigate the inrush current of the transformer. To this end, different magnetic materials used in the manufacturing of the transformer core, are considered and based on the related magnetic characteristic, the amplitude and the harmonic content of the produced inrush current are determined using EMTP-RV software. To select a suitable magnetic material for transformer core, a comparison among these magnetic materials is performed. In addition, other techniques used for mitigation of the transformer inrush current including the time of the transformer energizing, residual flux and transformer loading are used and their impact on the transformer inrush current is investigated using EMTP-RV software.

Keywords: core material comparison, EMTP-RV, inrush current, transformer switching strategy, magnetic characteristic, energizing time, residual flux effect

Corresponding Author: Dr. Amir Ghaedi
Corresponding Author Address: Department of Electrical Engineering- Dariun Branch -Islamic Azad University- Dariun, Iran

مطالعه جامع تکنیک های کاهش جریان هجومی ترانسفورماتور

امیر قائدی، دانشیار

گروه مهندسی برق، واحد داریون، دانشگاه آزاد اسلامی، داریون، ایران
amir.ghaedi@iau.ac.ir

تاریخ ارسال مقاله: ۱۴۰۴/۰۱/۳۰ **تاریخ بازنگری مقاله:** ۱۴۰۴/۰۵/۱۰ **تاریخ پذیرش مقاله:** ۱۴۰۴/۰۵/۲۵

چکیده: جریان هجومی ترانسفورماتور دارای دامنه بالا و جریان غیر سینوسی است که در سیکل‌های اولیه پس از برق‌رسانی به ترانسفورماتور رخ می‌دهد. این جریان ممکن است منجر به مشکلاتی در سیستم قدرت مانند افت ولتاژ، تلفات حرارتی، کاهش کیفیت توان و اختلال در عملکرد رله‌های حفاظتی شود. برای جلوگیری از عملکرد نادرست سیستم حفاظتی، مولفه‌های هارمونیک این جریان برای تشخیص این جریان از جریان‌های خطا مورد تجزیه و تحلیل قرار می‌گیرد. با این حال، تکنیک‌هایی که دامنه جریان هجومی ترانسفورماتور را کاهش می‌دهد می‌تواند از اثرات مخرب این جریان جلوگیری کند. برای این منظور، در این مقاله یک مطالعه جامع بر روی تکنیک‌های جدیدی که می‌توان برای کاهش جریان هجومی ترانسفورماتور استفاده کرد، انجام شده است. برای این منظور، مواد مغناطیسی مختلف مورد استفاده در ساخت هسته ترانسفورماتور در نظر گرفته شده و بر اساس مشخصه مغناطیسی مربوطه، دامنه و مولفه‌های هارمونیکی جریان هجومی تولید شده با استفاده از نرم افزار تحلیل حالت گذرای EMTP-RV تعیین می‌شود. برای انتخاب یک ماده مغناطیسی مناسب برای هسته ترانسفورماتور، مقایسه‌ای بین این مواد مغناطیسی انجام می‌شود. علاوه بر این، سایر تکنیک‌های مورد استفاده برای کاهش جریان هجومی ترانسفورماتور از جمله زمان انرژی‌دهی به ترانسفورماتور، شار باقی مانده و بارگذاری ترانسفورماتور مورد استفاده قرار می‌گیرد و تاثیر آن‌ها بر جریان هجومی ترانسفورماتور با استفاده از نرم افزار EMTP-RV بررسی می‌شود.

کلمات کلیدی: نرم‌افزار EMTP-RV، جریان هجومی، ترانسفورماتور، مشخصات مغناطیسی، زمان انرژی دهی، شار باقیمانده

نام نویسنده‌ی مسئول: دکتر امیر قائدی
نشانی نویسنده‌ی مسئول: داریون- دانشگاه آزاد اسلامی واحد داریون- دانشکده مهندسی برق

1. Introduction

The inrush current of the transformer is the large magnitude current produced in the initial cycles after energizing the transformer due to the nonlinear characteristic of the transformer magnetic core. Due to the large magnitude and long duration of this current, the protection system may malfunction and disconnect the transformer. In addition to the malfunction of the protection system, the inrush current causes problems such as voltage drop, heat losses and power quality effects. The magnitude of this current depends on different parameters such as the winding resistance, switching angle and residual flux density in the moment of energizing the transformer. To investigate the impact of the transformer inrush current on the power system, many researches have been performed to study the basis of inrush current production, the characteristics of this current, different techniques of distinguishing this current from the fault current and the methods for inrush current mitigation. In [1], the impact of inrush current on the transformer protection is evaluated. In this paper, using two case studies that were performed through the digital simulation technique based on the COMTRADE file, the effect of the transformer inrush current on the over-current protection and differential protection of the transformer is investigated. In [2], an improved design approach is proposed to reduce the inrush current of the transformer. In this paper, each phase of the transformer is energized in sequence and a neutral resistor is used to limit the inrush current of the three phase transformer. To determine the value of the neutral resistor for optimal performance, an analytical approach based on the nonlinear circuit transient analysis is developed. In [3], a new method based on box dimension is proposed to identify the transformer inrush current for preventing from mal-operation of the transformer differential protection. To distinguish the inrush current of the transformer from the inner fault currents, the fundamental difference in waveform between the two currents is utilized. Based on the proposed technique, the three-phase current is extracted and its box dimensions are calculated to identify the transformer inrush current. In [4], the simulation and experimental results associated to the sequential phase energizing method are given to reduce the inrush current of the transformer. In this paper, a grounding resistor connected to a transformer neutral point is used to act as a series-inserted resistor by energizing each phase of the transformer in sequence and significantly reduces the inrush current of the transformer. In [5], the impact of voltage across the breaker to be closed on the magnitude of the transformer inrush current is investigated. In this paper, based on the steady-state circuit theory, the proposed voltage is analysed and using the experimental results, the effectiveness of the method are satisfied. In [6], a dynamic model of the transformer is developed to predict the inrush current of the transformer produced from the arbitrary initial excitation of the transformer after the switch-off. The impact of the proposed model on the transient current overshoot, based on the residual magnetic flux prediction is investigated. In [7], a proper model is introduced for the ferromagnetic core of the transformer to consider the effects of the hysteresis, saturation, eddy current losses and anomalous losses of the transformer. In this paper, an artificial neural network is proposed to study the major DC hysteresis loop and initial magnetization curve of the transformer using experimental data. The proposed model of the ferromagnetic core is used to estimate the transformer inrush current. In [8], a new method is proposed to reduce the residual magnetic flux in the network transformer using a device composed of the low voltage DC source, suitable power electronic switching unit and a simple controller. In this paper, using time-domain simulation, it is proved that a small-power device can substantially reduce the residual magnetic flux of all transformer, simultaneously. In [9], a novel method based on the normalized grille curve is proposed to distinguish the inrush current of the transformer from the internal fault currents. In this paper, two schemes to distinguish the transformer inrush currents from the internal faults in the time and frequency domains are developed. Based on the 268 experimental measurement results on the YNd11-connected transformer, the effectiveness of the proposed method is satisfied. In [10], a new method based on the error estimation is proposed to identify the inrush current of the transformer from the internal fault currents. In this paper, based on the similarity between the actual wave and two reference waves under two different frequency condition per half cycle, the transformer inrush current is distinguished from the internal fault currents.

In [11-13], different techniques used to reduce the inrush current associated to the starting current of the electric motors are studied. In [11], the design of autotransformer and soft starter are focused in order to compare inrush current during the start-up three phase medium sized industrial induction motor by using MATLAB/Simulink software. Both starters were targeted to resolve the problems inherent in the dynamic operation of induction motors, which included current and torque surges during the motor start up. The autotransformer gives the choice to consumer in selecting different tap values, in which is the advantage to consumer to vary their starting current and starting torque according to its application. The aim of [12] is to address the selection, calculation and switching of the capacitor bank for reactive power compensation for inrush current of induction motors. This first requires the study of the reactive power drawn by an induction motor during starting. The capacitances are calculated and switched on to compensate the starting transient and disconnected when the machine has run up to speed using a point-on switching approach that reduces the switching transient. Paper [13] presents a new method of reducing the inrush current and improving the starting performance of a line-start permanent-magnet synchronous motor. The novelty of the proposed method relies on

the selection of the time instant of the connection of the stator winding to the grid, for which the smallest values of the amplitudes of inrush currents are obtained. To confirm the effectiveness of the developed method of limiting the inrush current, simulations and experimental studies were carried out.

Due to the problems arisen from the inrush current of the transformer, this paper proposes comprehensive approaches to reduce the inrush current of the transformer. At first, the materials used as magnetic core are studied and compared based on the inrush current they produced. This comparison can be used to select a suitable magnetic material as the magnetic core for inrush current reduction. Then, other parameters affected on the transformer inrush current are studied and the impact of them on the transformer inrush current is examined. Thus, the organization of this paper would be as bellows:

In the second section, the transformer inrush current is explained and different. In the third section, different magnetic materials used as magnetic core are introduced. The produced inrush currents associated to different magnetic materials are simulated using EMTP-RV software in the fourth section. The impact of other methods on the transformer inrush current is simulated in the fifth section. The paper is summarized in the sixth section.

2. Transformer inrush current

In this part, a single-phase transformer is considered to study the inrush current produced after energizing the transformer. In the energizing time of the transformer, the voltage of the primary winding of the transformer energized by the voltage source is considered to be:

$$v_1(t) = V_m \sin(\omega t + \theta) \Rightarrow v_1(0) = V_m \sin\theta \qquad (1)$$

Where, the θ is the initial angle of the voltage waveform at the energizing of the transformer. Based on the Faraday's law, the magnetic flux of the transformer core can be calculated as:

$$v_1(t) = N_1 \frac{d\phi}{dt} \Rightarrow \phi = \frac{1}{N_1}\int v_1(t)dt \qquad (2)$$

Where, N_1 is the number of turns of the primary winding. To calculate the value of the magnetic flux (ϕ), the initial magnetic flux or residual magnetic flux (ϕ_R) is added to the area below the voltage diagram as presented in Fig. 1.

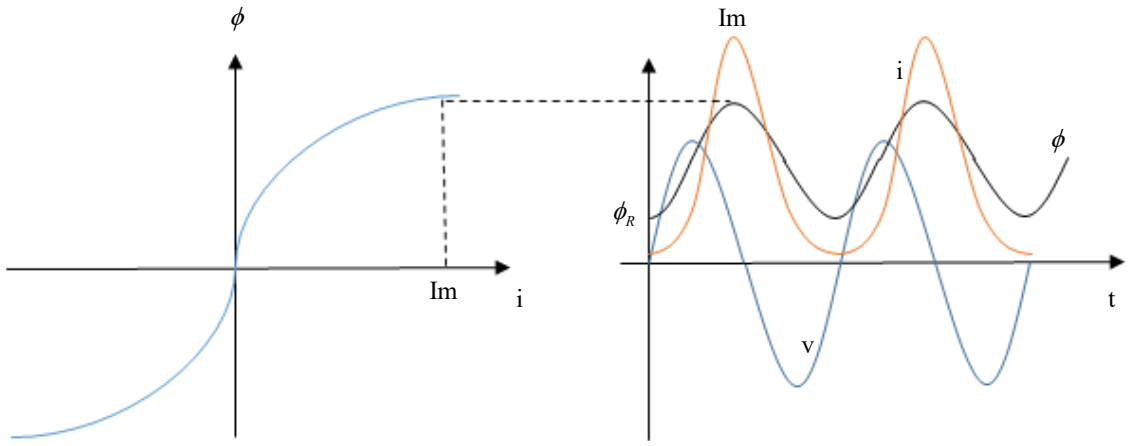

Fig. 1. The large inrush current of the transformer

According to the magnetic characteristic of the transformer core (magnetic flux-exciting current diagram) as presented in Fig. 1, in each time, based on the calculated magnetic flux, the associated current can be determined. As can be seen in the figure, if the magnitude of the calculated magnetic flux is large, the core is saturated and the associated current would be very large. Thus, the magnitude of the inrush current would be large and due to the nonlinear characteristic of the magnetic curve of the core arisen from the saturation of the core, the inrush current is non-sinusoidal and contains harmonic currents. If the switching time of the transformer is as presented in Fig. 2, and the residual flux is insignificant, the core works at linear region and is not saturated and so, the magnitude of the inrush current is not large and do not contain the harmonic currents. Thus, based on equation (1), if the initial angle of the voltage is 0° or 180°, the magnitude of the inrush current would be large; and if the initial angle of the voltage is 90° or 270°, the inrush current is symmetrical and its magnitude is low. In the switching time, the angle of the voltage may be between 0° and 360° and so, the inrush current magnitude would be determined based on the initial switching angle and residual flux.

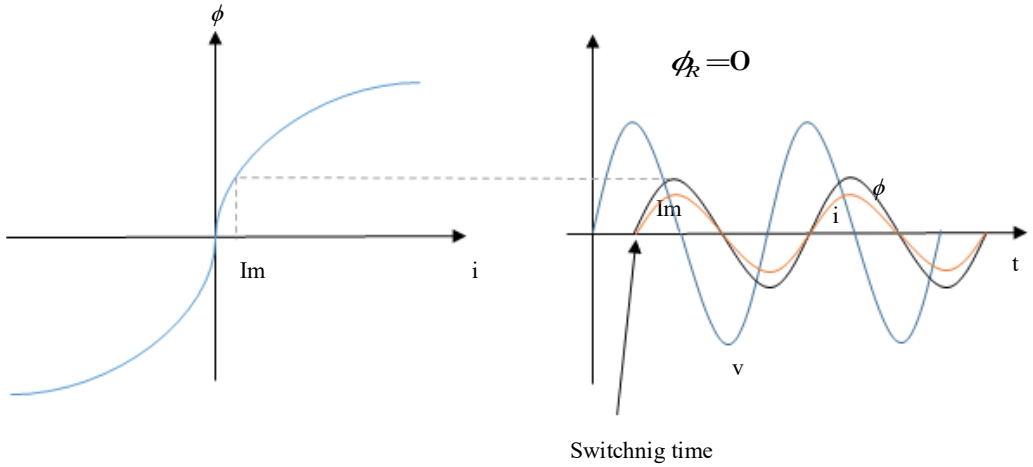

Fig. 2. The symmetrical inrush current of the transformer

As can be seen from the figures 1 and 2, the magnitude of the inrush current is dependent on the magnetic characteristic of the core (ϕ-i), the initial angle of the voltage in the switching time and the residual flux. Thus, to comprehensively study the transformer inrush current, the impact of the core magnetic characteristic, switching time and the residual flux on the transformer inrush current is investigated.

3. Different magnetic materials

In this section, the produced inrush current of the transformer associated to the different magnetic materials is studied. The magnetic materials play a key role in the design of the magnetic devices such as transformers, generators and electrical motors. To achieve an optimal design of the magnetic devise based on the cost, size and quality, different types of the magnetic materials such as silicon steel, nickel iron, cobalt iron, amorphous metallic alloy, ferrite, moly-perm alloy, sendust and iron powder can be used.

3.1. The characteristics of different magnetic materials

Due to the different application of magnetic devises, based on the desired characteristics from magnetic flux density value, saturation, permeability, core reluctance, resistance and losses, residual flux and coercivity points of view, the suitable magnetic material is selected. In this stage, 13 different magnetic materials including K-type ferrite at 25ºC, K-type ferrite at 100ºC, P&R-type ferrite at 25ºC, P&R-type ferrite at 100ºC, F-type ferrite at 25ºC, F-type ferrite at 100ºC, W&H-type ferrite at 25ºC, W&H-type ferrite at 100ºC, amorphous alloy 2714AF, moly perm alloy powder, high flux (HF) powder, sendust powder and 75 perm powder, are taken into consideration and the produced inrush currents of these materials are evaluated. The magnetic characteristic of these magnetic materials are presented in Fig. 3.

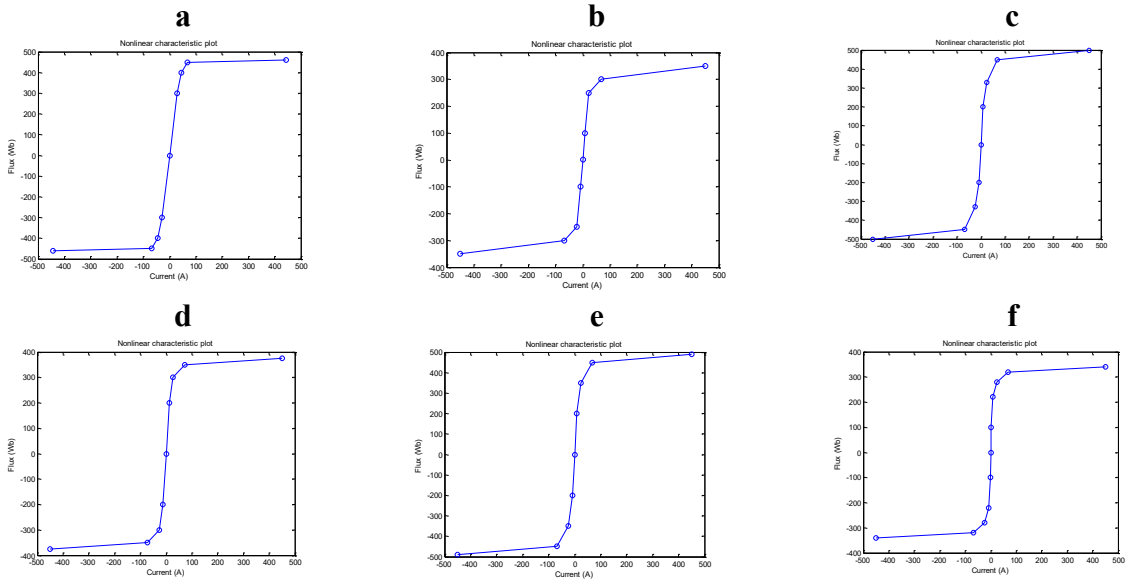

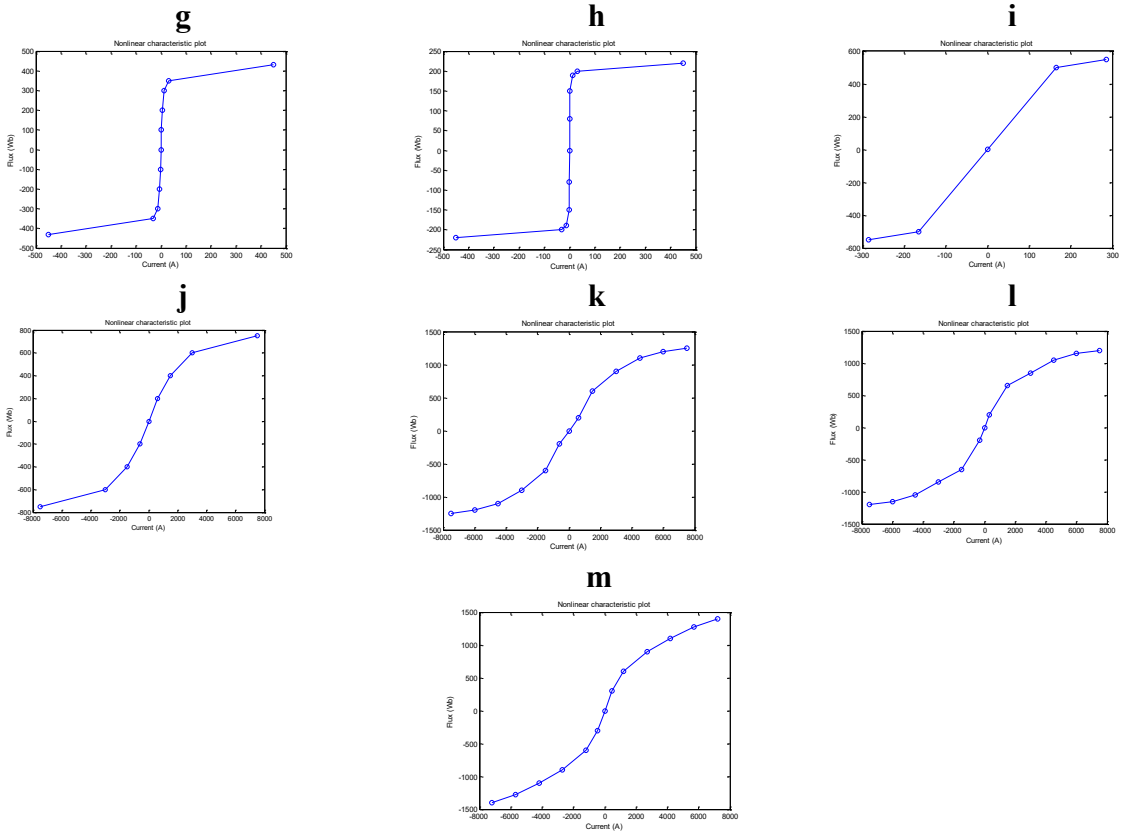

Fig. 3. The ϕ-i characteristic of magnetic materials, (a) *K-type ferrite at 25°C, (b) K-type ferrite at 100°C, (c) P&R-type ferrite at 25°C, (d) P&R-type ferrite at 100°C, (e) F-type ferrite at 25°C, (f) F-type ferrite at 100°C, (g) W&H-type ferrite at 25°C, (h) W&H-type ferrite at 100°C, (i) amorphous alloy 2714AF, (j) moly perm alloy powder, (k) high flux (HF) powder, (l) sendust powder and (m) 75 perm powder [14-18]*

3.2. The simulation results

To determine the inrush current of the transformer for different magnetic materials used as the magnetic core, using EMTP-RV software, a 230kv/66kv transformer is modeled as Fig. 4. The 230kv voltage source at 50Hz frequency is applied to the transformer. The impedance from the voltage source to the transformer is considered to be 0.2+j5 ohms. The series impedance of the transformer and the equivalent core resistance are considered to be 5+100j and 1058 ohms. The nonlinear characteristics of different materials are considered in the simulation process and the produced inrush currents for sinusoidal waveform of the voltage source (worst case) and no residual flux are determined and presented in Fig. 5. The harmonic currents of the produced inrush currents are determined using harmonic analysis of the associated inrush currents and presented in Fig. 6.

3.3. Discussion

To compare different magnetic materials used as the magnetic core of the transformer from the perspective of inrush current magnitude, the peak current magnitude, the main harmonic current magnitude, the magnitude of the second and third harmonics, the DC component of the inrush currents and the damping time associated to different magnetic materials are determined and presented in table 1.

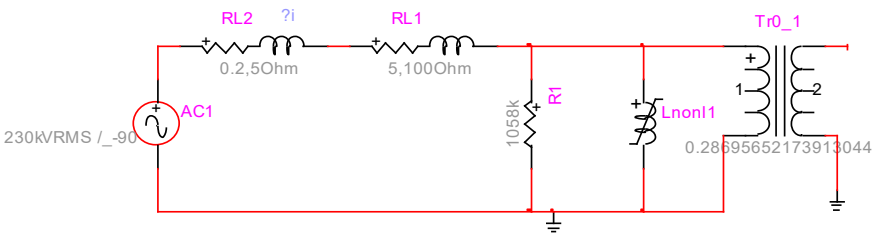

Fig. 4. The model of the transformer in the EMTP-RV software

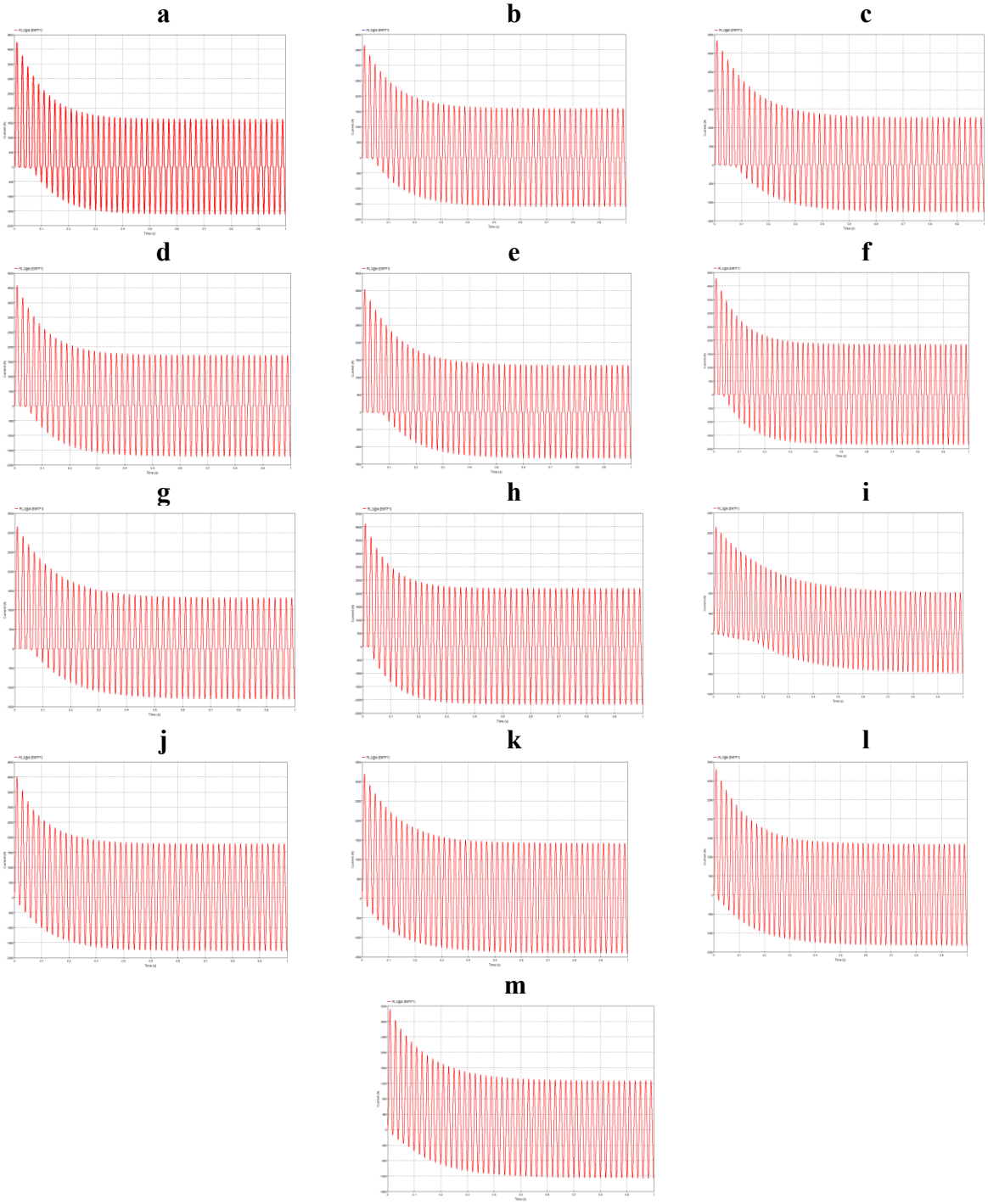

Fig. 5. The transformer inrush current associated to the different magnetic materials, (a) *K-type ferrite at 25°C, (b) K-type ferrite at 100°C, (c) P&R-type ferrite at 25°C, (d) P&R-type ferrite at 100°C, (e) F-type ferrite at 25°C, (f) F-type ferrite at 100°C, (g) W&H-type ferrite at 25°C, (h) W&H-type ferrite at 100°C, (i) amorphous alloy 2714AF, (j) moly perm alloy powder, (k) high flux (HF) powder, (l) sendust powder and (m) 75 perm powder*

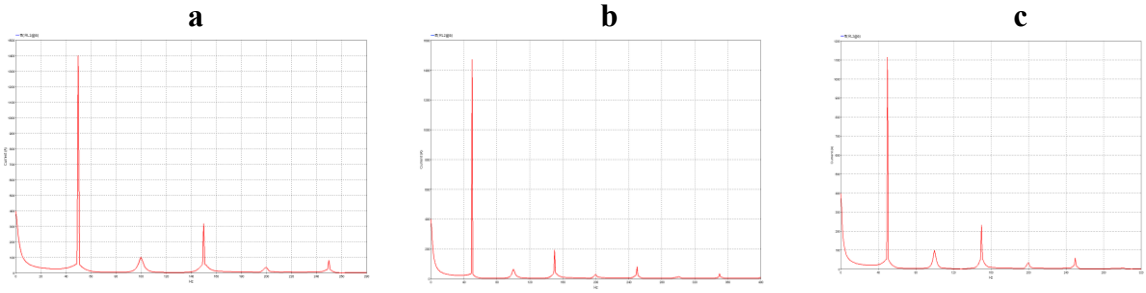

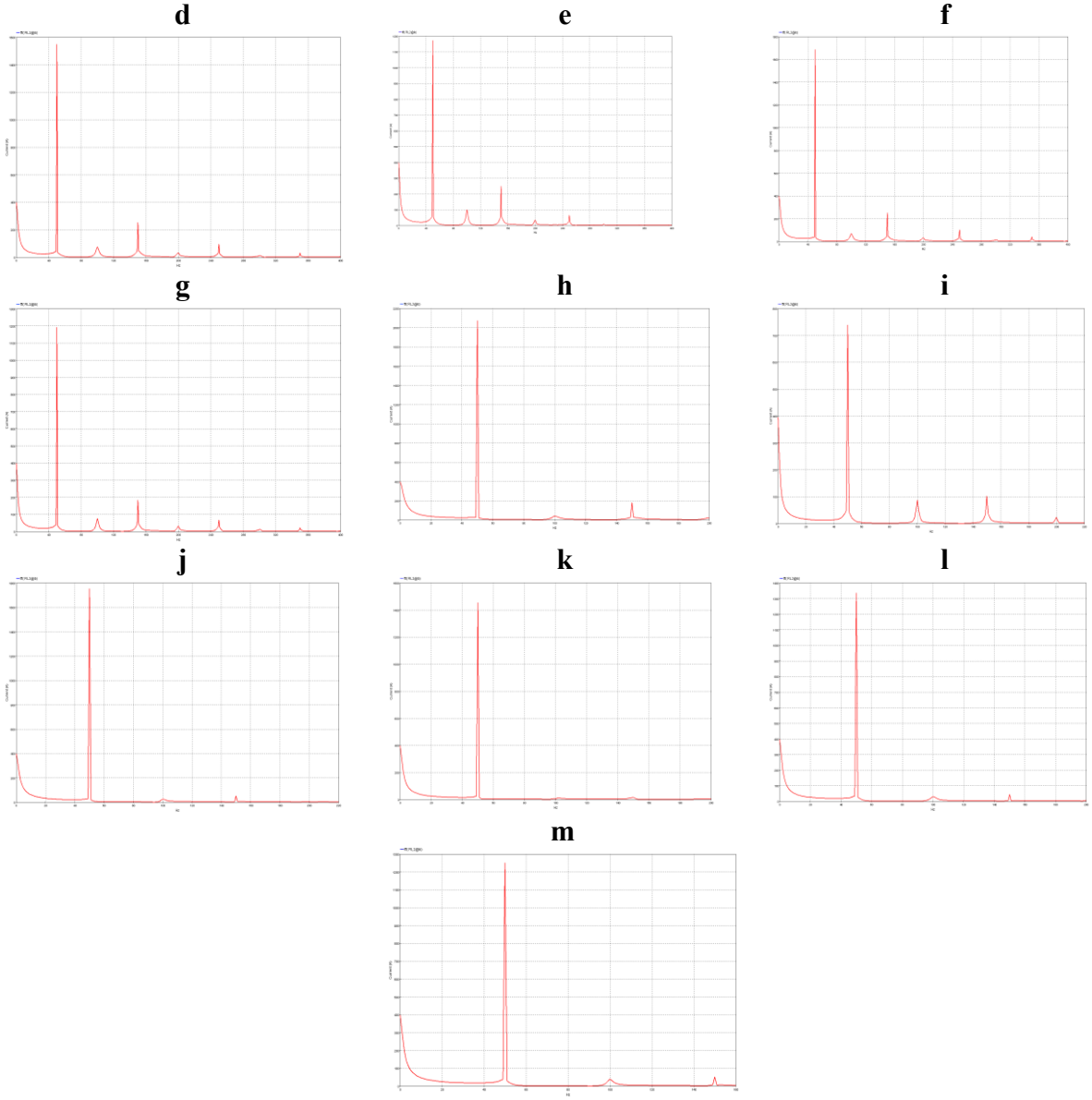

Fig. 6. The harmonic currents of the inrush current associated to the different magnetic materials, (a) *K-type ferrite at 25°C, (b) K-type ferrite at 100°C, (c) P&R-type ferrite at 25°C, (d) P&R-type ferrite at 100°C, (e) F-type ferrite at 25°C, (f) F-type ferrite at 100°C, (g) W&H-type ferrite at 25°C, (h) W&H-type ferrite at 100°C, (i) amorphous alloy 2714AF, (j) moly perm alloy powder, (k) high flux (HF) powder, (l) sendust powder and (m) 75 perm powder,*

Table. 1.The results of the simulation

material	Peak current (A)	Main harmonic (A)	2nd harmonic (A)	3rd harmonic (A)	Dc current (A)	Damping time
Ferrite K 25°C	4300	1400	100	320	400	0.4 S
Ferrite K 100°C	3700	1480	50	190	400	0.4 S
Ferrite P&R 25°C	3400	1120	100	240	400	0.6 S
Ferrite P&R 100°C	4100	1550	80	270	400	0.5 S
Ferrite F 25°C	3550	1180	100	260	400	0.5 S
Ferrite F 100°C	4300	1700	70	250	400	0.5 S
Ferrite W&H 25°C	3200	1190	80	190	400	0.6 S
Ferrite W&H 100°C	4600	2100	75	180	400	0.4 S
Amorphous 2714AF	2100	750	90	100	400	0.9 S
Moly perm alloy	4000	1780	30	50	400	0.6 S
high flux Powder	3200	1450	15	20	400	0.9 S
Sendust powder	3300	1350	30	50	400	0.6 S
75 perm powder	3150	1260	40	60	400	0.9 S

As can be seen from the figures and the table, among different magnetic materials, amorphous 2714AF produces the inrush current with the minimum magnitude. However, the time required to damp the produced inrush current is high in this case. Among these materials, the K-type ferrite (both 25ºC and 100ºC) and W&H-type ferrite (at 100ºC), have low damping times compared to the other materials. The DC components of all inrush currents are 400A. It is concluded from this analysis that the best magnetic material that can be used as magnetic core in the transformer based on the magnitude of the produced inrush current is amorphous 2714AF.

4. Other techniques for inrush current mitigation

In this section, the other factors affected to reduce the transformer inrush current including the angle of voltage at switching time, the residual flux and the load of the transformer are investigated and simulated using EMTP-RV software.

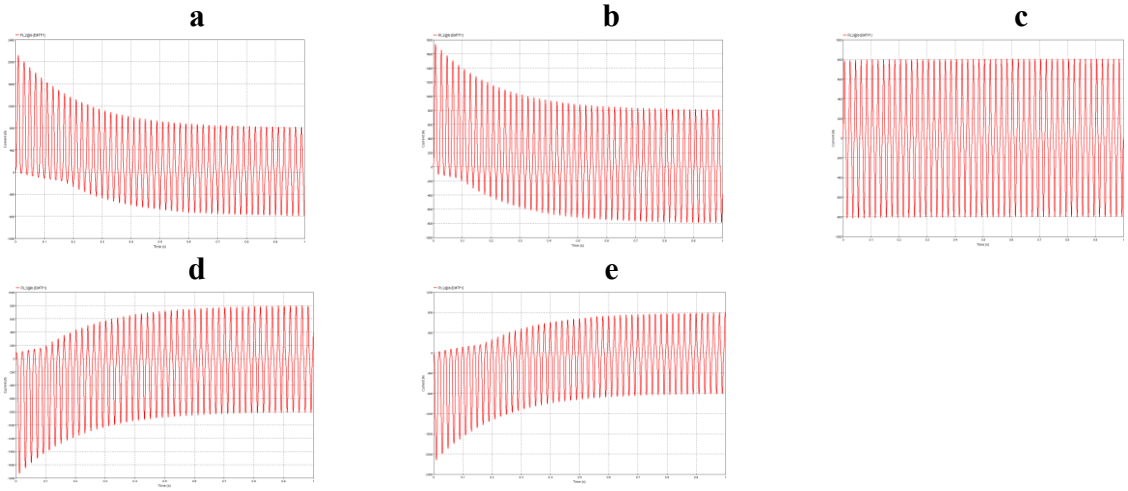

Fig. 7. The produced inrush current for initial angles of (a) 0º, (b) 45º, (c) 90º, (d) 135º and (e) 180º

4.1. The angle of voltage at the switching time

The magnetic flux of the transformer is determined by addition the residual flux to the area below the voltage diagram. If the voltage is sinusoidal waveform at the switching time, the area under voltage diagram from the angle of zero to π is positive and so, the produced flux would be large. However, if the angle of initial voltage is π/2, the area under the voltage diagram from zero to π/2 is positive and then is negative from π/2 to π. Thus, the inrush current associated to the sin-waveform is very large (worst case) and for the cosine-waveform is normal and symmetrical (best case). In this part, the understudied transformer equipped to the amorphous 2714AF is simulated using EMTP-RV software for different initial angle of the voltage applied to the transformer. In this stage, the residual flux is considered to be zero. The produced inrush current for different initial angles including 0, 45º, 90º, 135º and 180º are determined and presented in Fig. 7. The harmonic currents of the produced inrush currents for different initial angles of voltage are determined using harmonic analysis of the inrush currents and presented in Fig. 8.

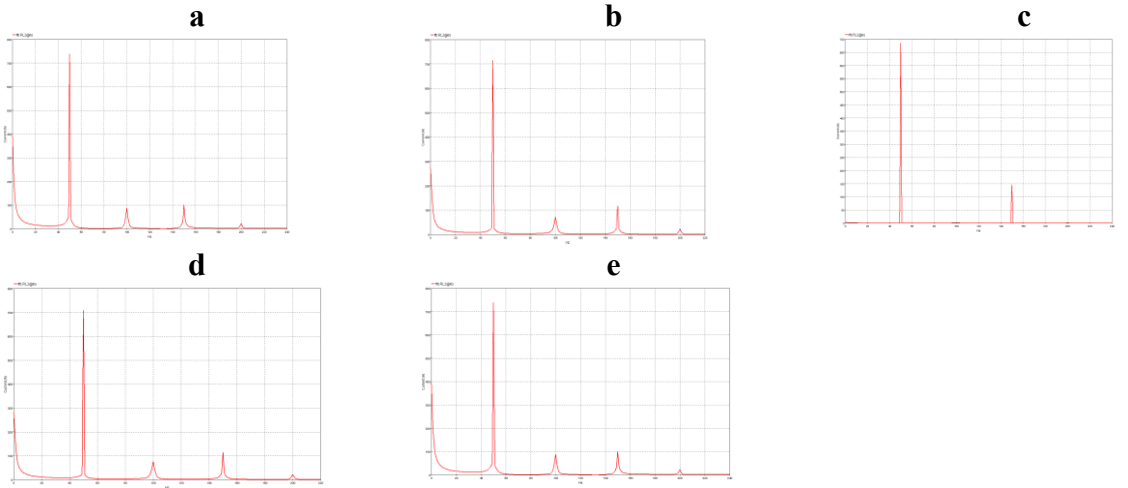

Fig. 8. The harmonic currents associated to the inrush current for initial angles of (a) 0º, (b) 45º, (c) 90º, (d) 135º and (e) 180º

The peak current, DC component, main harmonic magnitude, the second and third harmonics current magnitudes and the damping time associated to different initial angles of the voltage waveform are calculated and presented in table 2. As can be seen from the figures and the table, when the initial angles of the voltage waveform are 0^o or 180^o, the magnitude of the inrush current is very large (2100A) that is 2.625 times the inrush current associated to the best initial angles, i.e. the angles of 90^o or -90^0, that leads the inrush current magnitude is 800A. It is deduced from the table that the time required to damp the inrush current of the worst cases is 0.8 seconds that is equal to 40 cycles with the frequency of 50Hz.

Table. 2. The results of the simulation associated to the initial angle of the voltage

Switching angle (degree)	Peak current (A)	DC component (A)	Main harmonic (A)	2nd harmonic (A)	3rd harmonic (A)	Damping time (s)
0	2100	400	745	90	100	0.8
45	1750	280	710	80	110	0.6
90	800	0	680	0	150	0
135	-1750	280	710	80	110	0.6
180	-2100	400	745	90	100	0.8

4.2. The residual flux

In this subsection, the effect of the residual flux on the transformer inrush current is evaluated using EMTP-RV software. The magnetic flux of the transformer is determined by addition the residual flux to the area below the voltage diagram. If the signs of the residual flux and the variation in the produced magnetic flus are the same, the produced magnetic flux is added to the residual flux and the resulted magnetic flux would be larger. Thus, the produced inrush current is larger. However, if the produced magnetic flux results in the reduction of the residual flux, the generated magnetic flux would be smaller and so, the produced inrush current would be smaller. In this part, the initial angle of the voltage applied to the transformer equipped to the amorphous 2714AF magnetic core is considered to be 0^o. The produced inrush currents for different residual flux values including 0, -500Wb and 500Wb are determined using EMTP-RV software and presented in Fig. 9. The harmonic currents associated to these inrush currents are determined using harmonic analysis of the produced inrush currents and resented in Fig. 10. The peak current, DC component, main harmonic magnitude, the second and third harmonics current magnitudes and the damping time associated to different residual are calculated and presented in table 3. As can be seen from the figures and the table, when the residual flux is 500Wb that its sign and the sign of the magnetic flux change are the same, the magnitude of the inrush current is very large. However, if the residual flux is -500Wb, the produced magnetic flux that is positive is added to the residual flux and so, the total produced magnetic flux would be smaller than the cases with residual flux of zero and 500Wb. It is deduced from the table that the time required to damp the inrush current of the worst cases is more than 1 second that is more than 50 cycles with the frequency of 50Hz.

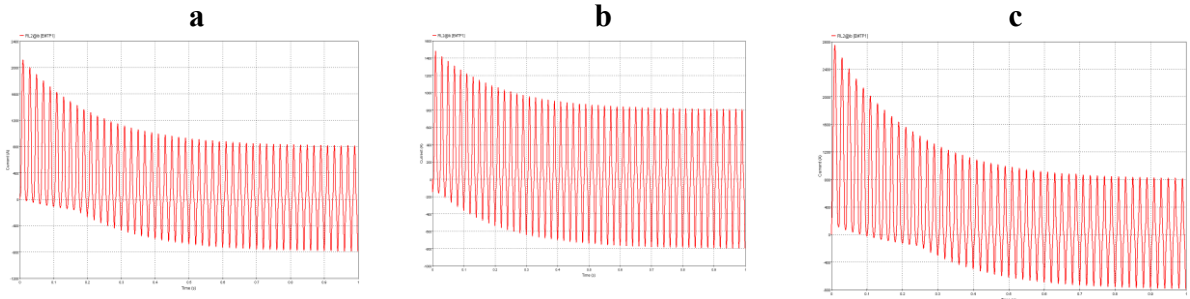

Fig. 9. The produced inrush current for residual flux values of (a) 0, (b) -500Wb, (c) 500Wb

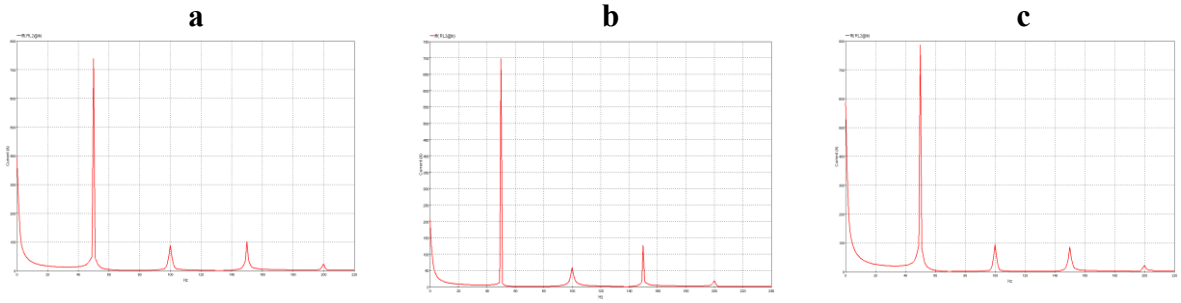

Fig. 10. The harmonic currents associated to the produced inrush currents for residual flux values of (a) 0, (b) -500Wb, (c) 500Wb

Table. 3. The results of the simulation associated to the residual flux

Residual flux (Wb)	Peak current (A)	DC component (A)	Main harmonic (A)	2nd harmonic (A)	3rd harmonic (A)	Damping time (s)
0	2100	400	745	90	100	0.9
-500	1500	200	700	60	130	0.8
500	2760	590	795	95	80	>1

4.3. The transformer loading

In this subsection, the effect of the transformer loading on the inrush current using EMTP-RV software is investigated. For this purpose, three different loads including no load, 15MW+j7MVAR and 45MW+j15MVAR are implemented on the transformer and the produced inrush currents for residual flux zero and the initial angle of 0° are determined and presented in Fig. 11. Using harmonic analysis, the harmonic currents associated to these inrush currents are determined and presented in Fig. 12. The peak current, DC component, main harmonic magnitude, the second and third harmonics current magnitudes and the damping time associated to different transformer loads are calculated and presented in table 4. As can be seen from the figures and the table, when the transformer is connected to the load, the magnitude of the produced inrush current is smaller and the time required to damp these currents is shorter. It is deduced from the numerical results that larger the load connected to the transformer, the smaller the produced inrush current magnitude and the shorter the damping time of the produced inrush current. Thus, it is suggested to energize the transformer under loads to reduce the produced inrush current of the transformer.

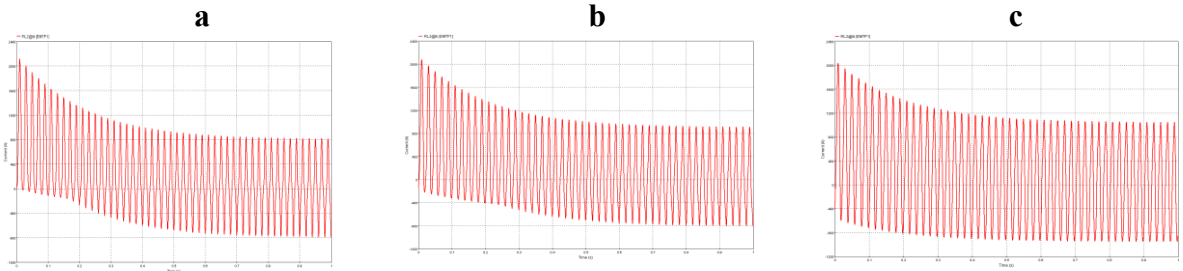

Fig. 11. The produced inrush current for different transformer loading (a) no load, (b) 15MW+j7MVAR and (c) 45MW+j15MVAR

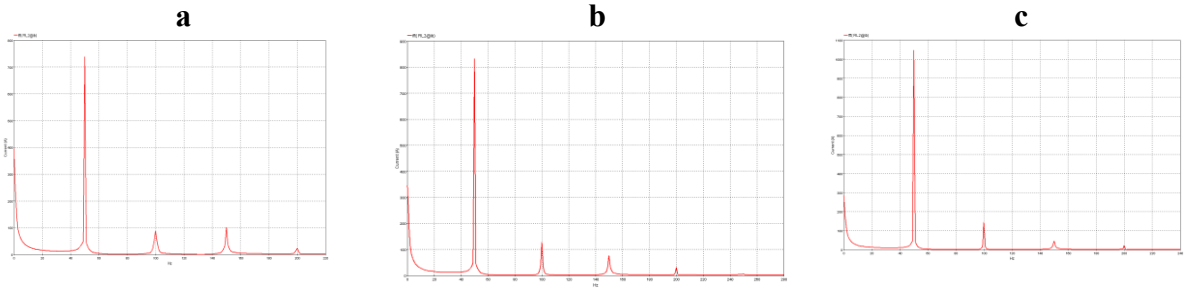

Fig. 12. The harmonic currents associated to the produced inrush currents for different transformer loading (a) no load, (b) 15MW+j7MVAR and (c) 45MW+j15MVAR

Table. 3. The results of the simulation associated to the different transformer loads

Load (MW,MVar)	Peak current (A)	DC component (A)	Main harmonic (A)	2nd harmonic (A)	3rd harmonic (A)	Damping time (s)
0	2100	400	745	90	100	0.9
15+7j	2050	350	840	120	80	0.8
45+15j	2020	290	1060	150	40	0.7

5. Conclusion

In this paper, the inrush current of the transformer resulted in the some challenges in the power system including the voltage drop, malfunction of the protective system, heat losses and power quality problems is studied. This current is dependent on the magnetic characteristic of the core, the angle of the voltage waveform applied to the transformer at the switching time, the residual flux and the load connected to the transformer. For this purpose, different magnetic materials including K-type ferrite at 25°C, K-type ferrite at 100°C, P&R-type ferrite at 25°C, P&R-type ferrite at 100°C, F-type ferrite at 25°C, F-type ferrite at 100°C, W&H-type ferrite at

25°C, W&H-type ferrite at 100°C, amorphous alloy 2714AF, moly perm alloy powder, high flux (HF) powder, sendust powder and 75 perm powder, are taken into consideration and based on the associated magnetic flux-current, the produced inrush currents of these materials are calculated using EMTP-RV software. It is concluded from the numerical results that among different magnetic material studied in the paper, the amorphous 2714AF is the best magnetic material that can be used as the magnetic core from the inrush current magnitude of the view. Then, the impact of the initial angle of the applied voltage on the transformer on the inrush current magnitude is evaluated and it is deduced that the best voltage waveform results in the minimum inrush current is the cosine-wave and the worst case results in the large inrush current is the application of the sin-wave on the transformer. The other factor studied in the paper is the residual flux of the core. It is deduced from the numerical results to reduce the inrush current of the transformer, the sign of the residual flux and the initial produced magnetic flux must be opposite. The third factor affected on the inrush current of the transformer that is investigated in this paper is the transformer loading. It is concluded from the numerical results that larger the load connected to the transformer, the smaller the produced inrush current magnitude and the shorter the damping time of the produced inrush current. Thus, it is suggested to energize the transformer under loads to reduce the produced inrush current of the transformer.

References

[1] Wu, Li-Cheng, et al. "The effect of inrush current on transformer protection." *2006 38th North American Power Symposium*. IEEE, 2006.

[2] Abdulsalam, Sami G., and Wilsun Xu. "Analytical study of transformer inrush current transients and its applications." *IPST Conference, Montreal, Canada*. 2005.

[3] Gong, Maofa, et al. "A Method for Identification of Transformer Inrush Current Based on Box Dimension." *Mathematical Problems in Engineering* 2017.

[4] Cui, Yu, et al. "A sequential phase energization technique for transformer inrush current reduction-Part I: Simulation and experimental results." *IEEE Transactions on power delivery*, vol. 20, no. 2, pp. 943-949, 2005.

[5] Xu, Wilsun, et al. "A sequential phase energization technique for transformer inrush current reduction-Part II: theoretical analysis and design guide." *IEEE transactions on power delivery*, vol. 20, no. 2, pp. 950-957, 2005.

[6] Cardelli, Ermanno, Antonio Faba, and Francesco Tissi. "Prediction and control of transformer inrush currents." *IEEE Transactions on Magnetics*, vol. 51, no. 3, pp. 1-4, 2015.

[7] Faiz, Jawad, and Saeed Saffari. "Inrush current modeling in a single-phase transformer." *IEEE Transactions on Magnetics*, vol. 46, no. 2, pp. 578-581, 2010.

[8] Kovan, Baris, et al. "Mitigation of inrush currents in network transformers by reducing the residual flux with an ultra-low-frequency power source." *IEEE Transactions on Power Delivery*, vol. 26, no. 3, pp. 1563-1570, 2011.

[9] Ma, Jing, et al. "Identifying transformer inrush current based on normalized grille curve." *IEEE Transactions on Power Delivery*, vol. 26, no. 2, pp. 588-595, 2011.

[10] He, Benteng, Xuesong Zhang, and Zhiqian Q. Bo. "A new method to identify inrush current based on error estimation." *IEEE Transactions on power delivery*, vol. 21, no. 3, pp. 1163-1168, 2006.

[11] Azizan, N. S., et al. "Medium sized industrial motor solutions to mitigate the issue of high inrush starting current." *AIP Conference Proceedings*. Vol. 2339. No. 1. AIP Publishing LLC, 2021.

[12] Habyarimana, Mathew, Remmy Musumpuka, and D. G. Dorrell. "Mitigating in-rush currents for induction motor loads." *2021 IEEE Southern Power Electronics Conference (SPEC)*. IEEE, 2021.

[13] Szelag, Wojciech, Cezary Jedryczka, and Mariusz Baranski. "A New Method of Reducing the Inrush Current and Improving the Starting Performance of a Line-Start Permanent-Magnet Synchronous Motor." *Energies*, vol. 17, no. 5, 1040, 2024.

[14] McLyman, Colonel Wm T. *Transformer and inductor design handbook*. CRC press, 2017.

[15] Chan, H. L., et al. "Study on magnetic materials used in power transformer and inductor." *2006 2nd International Conference on Power Electronics Systems and Applications*. IEEE, 2006.

[16] Hilzinger, Rainer, and Werner Rodewald. *Magnetic materials: fundamentals, products, properties, applications*. Vacuumschmelze, 2013.

[17] EPCOS, AG. "Ferrites and accessories-SIFERRIT material N87." *Data Sheet, September* 2006.

[18] Handbook, Ferroxcube Data. "Soft Ferrites and Accessories.", 95, 2009.